Bruno Bühler ORCID iD: 0000-0001-6458-5739

Constitutively solvent-tolerant *Pseudomonas taiwanensis* VLB120Δ*C*Δ*ttgV* supports particularly high styrene epoxidation activities when grown under glucose excess conditions

Running title: Solvent tolerance promotes biocatalytic epoxidation

Jan Volmer[1]*, Martin Lindmeyer[1,2]*, Julia Seipp[1], Andreas Schmid[2], Bruno Bühler[2#]

Affiliation:

[1]Department of Biochemical and Chemical Engineering, TU Dortmund University, Dortmund, Germany

[2]Department of Solar Materials, Helmholtz Centre for Environmental Research GmbH – UFZ, Leipzig, Germany

*Jan Volmer and Martin Lindmeyer contributed equally to this work

Correspondence to:

Bruno Bühler, Department of Solar Materials, Helmholtz Centre for Environmental Research GmbH – UFZ, Permoserstrasse 15, 04318 Leipzig, Germany

Email: bruno.buehler@ufz.de; Tel.: +49 341 235 46 87; Fax: +49 341 235 45 12 86

Funding information:

Ministry of Innovation, Science, and Research of North Rhine-Westphalia (CLIB-Graduate Cluster Industrial Biotechnology, CLIB2021), Grant/Award Number: Jan Volmer; German Federal Ministry of Education and Research (ERA-IB project "*Pseudomonas* 2.0"), Grant/Award Number: EIB.10.041.

Abstract

Solvent-tolerant bacteria represent an interesting option to deal with substrate and product toxicity in bioprocesses. Recently, constitutive solvent tolerance was achieved for *Pseudomonas taiwanensis* VLB120 via knockout of the regulator TtgV, making tedious adaptation unnecessary. Remarkably, *ttgV* knockout increased styrene epoxidation activities of *P. taiwanensis* VLB120Δ*C*. With the aim to characterize and exploit the biocatalytic potential of *P. taiwanensis* VLB120Δ*C* and VLB120Δ*C*Δ*ttgV,* we investigated and correlated growth physiology, native styrene monooxygenase (StyAB) gene expression, whole-cell bioconversion kinetics, and epoxidation performance. Substrate inhibition kinetics was identified, but was attenuated in two-liquid phase bioreactor setups. StyA-eGFP fusion enabled precise enzyme level monitoring without affecting epoxidation activity. Glucose limitation compromised *styAB* expression and specific activities (30-40 U g_{CDW}^{-1} for both strains), whereas unlimited batch cultivation enabled specific activities up to 180 U g_{CDW}^{-1} for VLB120Δ*C*Δ*ttgV* strains, which is unrivaled for bioreactor-based whole-cell oxygenase biocatalysis. These extraordinarily high specific activities of constitutively solvent-tolerant *P. taiwanensis* VLB120Δ*C*Δ*ttgV* could be attributed to its high metabolic capacity, which also enabled high expression levels. This together with the high product yields on glucose and biomass obtained qualifies the VLB120Δ*ttgV* strain as a highly attractive tool for the development of eco-efficient oxyfunctionalization processes and redox biocatalysis in general.

Graphical Abstract

Solvent-tolerant bacteria represent an interesting option to deal with substrate and product toxicity in bioprocesses. Recently, constitutive solvent tolerance was achieved for *Pseudomonas taiwanensis* VLB120 via knockout of the regulator TtgV, making tedious adaptation unnecessary.

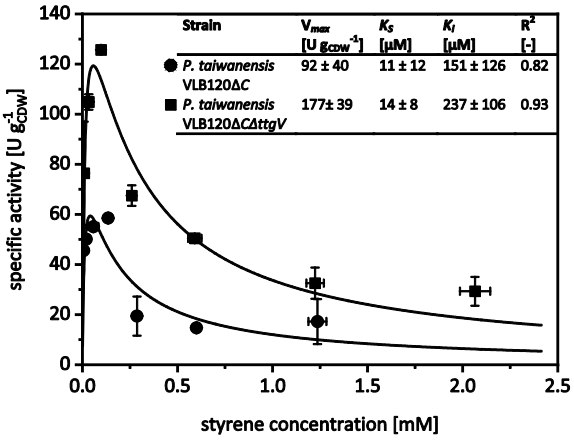

Keywords: Biocatalytic oxyfunctionalization, solvent tolerance, *Pseudomonas*, biochemical engineering, energy metabolism, styrene epoxidation

Introduction

The development of biotechnological processes in the chemical industry is constantly intensified, driven by inherent advantages like specificity, energy efficiency, and resource use (Clomburg et al., 2017; Schrewe et al., 2013; Sheldon and Woodley, 2017; Woodley et al., 2013). Especially the biotechnological production of fine chemicals and pharmaceuticals is well established and can already be economically and ecologically competitive to existing chemical syntheses (Kuhn et al., 2010; Woodley et al., 2013). However, involved substrates and products often are toxic towards microorganisms, which needs to be dealt with by reaction engineering and/or the use of solvent-tolerant bacteria (Heipieper et al., 2007).

The biocatalytic production of enantiopure (*S*)-styrene oxide, which is difficult to achieve by chemical means (Besse and Vaschambre, 1994), constitutes a prominent and well investigated example for such a process, in which the application of an extractive second liquid phase enabled high productivities. Thereby, the two-component styrene monooxygenase StyAB, originating from *Pseudomonas taiwanensis* VLB120 (Köhler et al., 2013; Panke et al., 1998), catalyzes styrene epoxidation in recombinant *E. coli* JM101 with an enantiomeric excess ≥ 99.7% (Kuhn et al., 2012b; Panke et al., 1998; Schmid et al., 2001). A highly efficient process was developed and applied up to a 30 L pilot scale, proving its competitiveness with existing chemical processes in economic and ecological assessments (Kuhn et al., 2012b; Kuhn et al., 2010; Panke et al., 2002; Panke et al., 2000; Park et al., 2006). Nevertheless, the application of recombinant *E. coli* came along with some disadvantages. Also in the presence of an extractive phase, (*S*)-styrene oxide toxicity remained a main limiting factor, leading to inhibition and permeabilization of the cells, coming along with a loss in activity and the formation of acetate as a stress response (Julsing et al., 2012; Kuhn et al., 2012b; Park et al., 2006). Furthermore, 2-phenyl ethanol accumulated as by-product promoting toxification and complicating downstream processing (Panke et al., 2000; Park et al., 2006). The construction of a styrene oxide isomerase deficient mutant of solvent-tolerant *P. taiwanensis* VLB120 allowed the application of StyAB in its native environment and the avoidance of by-product accumulation (Park et al., 2007). The achieved process performance indeed indicated a higher tolerance of *P. taiwanensis* VLB120Δ*C* towards (*S*)-styrene oxide compared to *E. coli* JM101 (pSPZ10) (Kuhn et al., 2012a). However, the increased biocatalyst stability was antagonized by decreased specific epoxidation activities as well as reduced overall biomass and (*S*)-styrene oxide yields on glucose (Kuhn et al., 2012a). As a possible cause, a competition for energy

between maintenance, solvent tolerance mechanisms, and styrene epoxidation was discussed. High energy demands to establish solvent tolerance have been identified earlier as a critical aspect in the application of solvent-tolerant *Pseudomonas* strains (Blank et al., 2008b; Isken et al., 1999; Meyer et al., 2006; Volmer et al., 2014). Yet, the knockout of a transcriptional repressor of solvent efflux pump gene expression not only led to a constitutively solvent-tolerant phenotype, but also to a doubling of styrene epoxidation activities (Volmer et al., 2014; Volmer et al., 2017). Further, the constitutive solvent tolerance of the resulting mutant strain VLB120Δ*C*Δ*ttgV* could be exploited to reduce the amount of the carrier solvent BEHP, which reduced environmental impact and costs of the process (Volmer et al., 2017). However, the interrelation of constitutive solvent tolerance and epoxidation activities and the resulting application potential of the Δ*ttgV* strain remained unclear.

In this study, the positive influence of the constitutive solvent tolerance of *P. taiwanensis* VLB120Δ*C*Δ*ttgV* on the biocatalytic performance and respective limiting factors were investigated under process conditions by means of gene expression and kinetic analyses as well as energy-limited and non-limited cultivation setups. For expression analysis, a genomic *styA-eGFP* fusion was established, a strategy applied before to quantify plasmid-based expression in different *Pseudomonas putida* strains (Lindmeyer et al., 2015a). To evaluate process performance characteristics of the VLB120Δ*C*Δ*ttgV* strain, specific activities, volumetric productivities, as well as biomass and product yields on glucose were determined and compared to those obtained with the VLB120Δ*C* strain and recombinant *E. coli* JM101.

Materials and methods

Bacterial strains, plasmids, and DNA manipulation

Bacterial strains and plasmids used in this study are listed in Table I. For the construction of the plasmid pEMG-A-eGFPB, *styA-eGFP* was amplified via PCR from pSMART-HCKan_StyA-eGFPB using primers F1 and B1 (Table S1) and ligated into pEMG as a *Sac*I/*Xba*I fragment using *E. coli* DH5α λpir (Martinez-Garcia and de Lorenzo, 2011). pEMG-A-eGFPB was then used for genomic integration of the *StyA-eGFP* fusion into *P. taiwanensis* VLB120ΔC and VLB120Δ*C*Δ*ttgV* applying the pEMG/pSW-2 method (Martinez-Garcia and de Lorenzo, 2011).

Media and growth conditions

Precultivations were carried out in LB medium (Bertani, 1951). Second pre- and main cultivations were carried out in M9 medium (Sambrook and Russel, 2001). For two-liquid phase biotransformations, modified Riesenberg (RB) medium was applied with 0.5-2% (w/v) glucose as sole carbon source (Bühler et al., 2003; Riesenberg et al., 1991). For pseudomonads, RB medium without citrate was applied to avoid respective regulatory effects. RB medium allowed cultivating VLB120 strains on glucose without intermediary gluconate accumulation (Volmer et al., 2017). The pH in M9 and RB media was adjusted to 7.2 and 6.8, respectively using 25% NH_4OH. In RB medium, it was further adjusted to 7.2 using 10 M NaOH. Antibiotics (50 µg mL^{-1} kanamycin, 50 µg mL^{-1} gentamycin, 100 µg mL^{-1} streptomycin) and 1 mL L^{-1} 1% (w/v) thiamine solution were supplemented if required. Cultivations were performed in baffled, screw-capped Erlenmeyer flasks at a gas:liquid ratio of 9:1 (v/v), 200 rpm (25 mm amplitude), and 30 °C.

Induction kinetics and whole-cell activity assays with nitrogen-limited resting cells

Induction of *styAB* gene expression was evaluated with styrene, (*S*)-styrene oxide, and 1-phenyl-1,2-ethandiol as inducing agents, which were added to a final concentration of 2 mM. Samples for fluorescence and GC-measurements were taken regularly for 4 h. Resting-cell activity assays with 5 min reaction time were carried out in 0.1 M potassium phosphate buffer (pH 7.4) containing 1% (w/v) glucose as described before (Volmer et al., 2014).

Two-liquid phase biotransformation

Two-liquid phase biotransformations were carried out in a 3.1 L stirred-tank KLF2000 bioreactor (Bioengineering, Wald, Switzerland) as described previously (Kuhn et al., 2012a; Kuhn et al., 2012b; Volmer et al., 2017). In short, biotransformations based on batch cultures (1 L RB medium, 30°C, pH = 7.2, 20 g L^{-1} glucose, 1 vvm) were started, when a biomass concentration of 0.5 g_{CDW} L^{-1} was reached, by addition of well-mixed 920 mL BEHP and 80 mL styrene and continued until glucose was depleted. For biotransformations based on fed-batch cultures, batch cultivation was followed by exponential feeding of a solution containing 730 g L^{-1} glucose and 19.6 g L^{-1} $MgSO_4 \cdot 7\ H_2O$ for a specific growth rate μ of 0.1 h^{-1}, until a biomass concentration of 20 g_{CDW} L^{-1} was reached. Then the organic phase (920 mL BEHP, 80 mL styrene) was added and the feed was kept constant at 7.8 g_{Glc} h^{-1}, until styrene was depleted. *E. coli* (pA-EGFP_B_lac) was induced by the addition of 1 mM IPTG upon organic phase addition. Sample preparation was carried out as described earlier (Kuhn et al., 2012b; Panke et al., 1999). For eGFP fluorescence analysis, an additional sample was taken, of which cells were resuspended to a concentration of ~0.1 g_{CDW} L^{-1} in PBS

buffer (145 mM NaCl, 1.8 mM $NaH_2PO_4 \cdot H_2O$, 6 mM Na_2HPO_4) containing 10% (v/v) glycerol and stored at -20 °C.

Determination of styrene epoxidation kinetics

The kinetic parameters for styrene epoxidation by *P. taiwanensis* VLB120Δ*C* and VLB120Δ*C*Δ*ttgV* were determined in 5 min resting-cell assays, which were carried out in 0.1 M potassium phosphate buffer (pH 7.4) containing 1% (w/v) glucose as described before (Volmer et al., 2014), applying the following styrene concentrations: 0.023, 0.047, 0.094, 0.188, 0.375, 0.75, 1.5, and 2.25 mM. Whole-cell kinetic parameters were estimated utilizing Equation 1 for substrate inhibition kinetics (Copeland, 2000; Cornish-Bowden, 1995):

Equation 1 $$v = \frac{V_{max}}{1+\frac{K_S}{[S]}+\frac{[S]}{K_i}}$$

Thereby, the reaction rate v depends on the maximum reaction rate V_{max}, the substrate concentration [S], the substrate uptake constant K_S, and the inhibition constant K_i. A least-square fit algorithm was used to perform nonlinear regression using GraphPad Prism 6.05 (GraphPad Software, La Jolla, CA, USA).

Analytics

Cell dry weight (CDW) concentrations were determined by measuring the optical density at 450 nm (OD_{450}) using a Libra S11 spectrophotometer (Biochrom Ltd., Cambridge, UK) and a correlation factor of 0.186 and 0.166 $g_{CDW}\ L^{-1}\ OD_{450}^{-1}$ for *P. taiwanensis* and *E. coli*, respectively (Blank et al., 2008a; Halan et al., 2010). GC and HPLC analyses for the quantification of styrene/ (*S*)-styrene oxide and glucose/ gluconate/ acetate, respectively, were performed as described before (Kuhn et al., 2010). Specific eGFP fluorescence was measured in microtiter plates using an Infinite

M200 reader (Tecan, Mannedorf, Switzerland) following a proceeding reported before (Lindmeyer et al., 2015a).

Results

StyA-eGFP fusion reveals differing StyAB expression levels for VLB120Δ*C* and VLB120Δ*C*Δ*ttgV* strains.

In order to investigate the *styAB* expression in the *P. taiwanensis* strains VLB120Δ*C* and VLB120Δ*C*Δ*ttgV*, the *styA* gene encoding the oxygenase component was replaced by a *styA-eGFP* fusion construct, giving rise to the *P. taiwanensis* strains VLB120Δ*C_AeGFP* and VLB120Δ*C*Δ*ttgV_AeGFP*. StyA was chosen as fusion target, as it harbors the active site and is the first gene of the *sty*-operon minimizing the transcriptional delay (Lim et al., 2011). Fluorescence measurements and sequence analyses confirmed the correct genomic *styA* gene replacements. Growth physiologies of VLB120Δ*C_AeGFP* (μ = 0.49 ± 0.01 h^{-1}, $Y_{X/S}$ = 0.36 g_{CDW} g_{glc}^{-1}) and VLB120Δ*C*Δ*ttgV_AeGFP* (0.48 ± 0.01 h^{-1}, 0.36 g_{CDW} g_{glc}^{-1}) in glucose containing M9 medium were similar and comparable to those of the respective parental strains (Volmer et al., 2014). The genetic modifications obviously did not significantly influence cellular metabolism. Upon induction by 2 mM styrene or styrene oxide, the VLB120Δ*C*Δ*ttgV_AeGFP* strain showed 1.5- to 2-fold higher intracellular StyA-eGFP levels than VLB120Δ*C_AeGFP* (Fig. S1). In accordance to previous results (Volmer et al., 2014), styrene-induced VLB120Δ*C*Δ*ttgV* cells showed ~2.6 times higher specific activities than the parent VLB120Δ*C* strains in resting-cell assays (Figs. 1 and S2). Cells harboring the fusion construct and the native s*tyAB* genes showed similar specific activities (Fig. S2), indicating that epoxidation activities are not affected by the fusion of *eGFP* to *styA*, as it has been observed before for plasmid-based expression controlled by the *alk*-regulatory system in *E. coli* and *Pseudomonas*

strains (Lindmeyer et al., 2015a). The activity difference among the strains containing the StyA-eGFP fusion correlated qualitatively but not quantitatively with the difference in specific fluorescence, revealing a higher expression level as one but possibly not the only reason for the higher activity of Δ*ttgV* strains.

Styrene epoxidation with *P. taiwanensis* strains is subject to substrate inhibition. To determine, whether styrene epoxidation is inhibited by high aqueous styrene concentrations as indicated by increased specific epoxidation activities at low aqueous styrene concentrations (results not shown) and in *in vitro* experiments (Ruinatscha, 2009), the styrene epoxidation kinetics of *P. taiwanensis* VLB120Δ*C* and VLB120Δ*C*Δ*ttgV* were analyzed in resting-cell assays (Fig. 1). Styrene epoxidation activities indeed followed substrate inhibition-type kinetics, although the low R^2-values and thus relatively high standard deviations for the kinetic parameters indicate that kinetics do not exactly follow Equation 1. Similarly to the epoxidation activities in resting-cell assays reported above (Fig. S2), the theoretical V_{max} of *P. taiwanensis* VLB120Δ*C*Δ*ttgV* was around two-fold higher than that of *P. taiwanensis* VLB120Δ*C*. Remarkably, the obtained K_S values were in the same range as the K_m value reported for isolated StyAB (0.02 mM; Ruinatscha, 2009). Slightly higher K_S and K_i values were found for *P. taiwanensis* VLB120Δ*C*Δ*ttgV*, which can be explained by continuous styrene extrusion by solvent efflux pumps in the constitutively solvent-tolerant mutant strain. The strong substrate inhibition of *P. taiwanensis* VLB120Δ*C* and also VLB120Δ*C*Δ*ttgV* (despite its constitutive solvent tolerance) asks for a setup enabling controlled substrate supply such as two-liquid phase systems with an organic phase serving as substrate reservoir.

Two-liquid phase biotransformations with *P. taiwanensis* VLB120 strains cultivated in fed-batch mode appear to be energy-limited. In order to characterize and compare gene expression and catalytic performance of the *P. taiwanensis* strains VLB120Δ*C_AeGFP* and *P. taiwanensis* VLB120Δ*C*Δ*ttgV_AeGFP* under process conditions, high-cell-density fed-batch cultivations were performed utilizing the optimized two-liquid phase process setup reported before (Kuhn et al., 2012a). Biotransformations were started via organic phase addition, when a cell concentration of ~20 g_{CDW} L^{-1} was reached. A limiting glucose feed (7.8 g_{Glc} h^{-1}) was constantly applied during the biotransformation to prevent glucose accumulation and ensure comparability to previous experiments with *E. coli* JM101 (pSPZ10) and *P. taiwanensis* VLB120Δ*C* (Kuhn et al., 2012a; Kuhn et al., 2010).

Under these conditions, *P. taiwanensis* VLB120Δ*C*Δ*ttgV_AeGFP* did not show higher epoxidation activities than the VLB120Δ*C_AeGFP* strain (Fig. 2), which was in contrast to their behavior in resting cell assays (Fig. S2) and in two-liquid phase batch cultures of the Δ*C* and Δ*C*Δ*ttgV* strains (Volmer et al., 2017). After 3 h, both strains reached a maximal activity of 30-40 U g_{CDW}^{-1}, which decreased towards the end of the biotransformation. Also StyA-eGFP expression levels did not differ among the two strains. After an initial parallel increase in expression levels and specific activities, only an increase in StyA_eGFP levels persisted surpassing the levels within cells used in resting-cell experiments, where higher activities up to 120 U g_{CDW}^{-1} were observed (Figs. 1, S1, S2). These results indicate that intracellular oxygenase concentrations did not limit styrene epoxidation.

After organic phase addition, growth of the VLB120Δ*C*Δ*ttgV_AeGFP* strain was more severely affected leading to a final biomass concentration (30 g_{CDW} L^{-1}), which was 25% lower compared to VLB120Δ*C_AeGFP* (Table II). The process performance

obtained with the VLB120Δ*C_AeGFP* strain was nearly identical to that reported for *P. taiwanensis* VLB120Δ*C* (Kuhn et al., 2012a) confirming the negligible influence of eGFP fusion. Overall, 62 and 58% of the initially added styrene were converted into (*S*)-styrene oxide by the VLB120Δ*C_AeGFP* and VLB120Δ*C*Δ*ttgV_AeGFP* strains, respectively (Table II). The decrease in the sum of styrene and (*S*)-styrene oxide concentrations can be ascribed to loss of styrene via evaporation and the degradation of the by-product phenyl acetaldehyde as described before (Hofstetter et al., 2004; Kuhn et al., 2012a).

The low styrene epoxidation activities observed during fed-batch cultivation, although low aqueous styrene concentrations and high intracellular StyAB monooxygenase levels were maintained, points towards a negative impact of glucose and thus energy limitation on the epoxidation capacity of *P. taiwanensis* VLB120Δ*C* strains.

Under glucose-excess conditions, *P. taiwanensis* VLB120 strains enable high styrene epoxidation activities in two-liquid phase biotransformations. Nitrogen-limited resting cells (Fig. 1) and cells grown in batch mode (Volmer et al., 2017) showed significantly higher maximum activities than cells cultivated in fed-batch mode (Fig. 2). To figure out, whether this difference can be attributed to the differing glucose availability and/or differing StyAB expression levels, two-liquid phase biotransformations were carried out under glucose excess conditions with cells cultivated in batch mode. When a cell concentration of 0.5 g_{CDW} L^{-1} was reached, biotransformations were started by organic phase addition.

P. taiwanensis strains VLB120Δ*C_AeGFP* and VLB120Δ*C*Δ*ttgV_AeGFP* exhibited specific epoxidation activities of up to ~110 and ~180 U g_{CDW}^{-1}, respectively, which were maintained until glucose depletion (Fig. 3). Almost all process performance

parameters were improved compared to fed-batch cultivation, except for the average productivity, which was reduced ~2-fold due to the 7-20-fold lower cell concentration applied (Table III). For both strains, specific eGFP fluorescence increased continuously throughout the biotransformation and reached a 1.5- and 2.3-fold higher level than in fed-batch cultivations of Δ*C* and Δ*C*Δ*ttgV* strains, respectively. Concomitantly, however, maximal specific activities were 3.1- and 5.1-fold higher, respectively. As in fed-batch cultures, StyA-eGFP levels continued to increase, after specific epoxidation activities had reached a maximum. The higher oxygenase expression levels and, especially, the higher activities reached under glucose excess conditions compared to those reached under glucose-limited conditions confirm that glucose and thus energy availability plays a crucial role for the exploitation of the very high epoxidation capacity of *P. taiwanensis* VLB120 strains.

The biocatalytically more active VLB120Δ*C*Δ*ttgV* strains showed a more pronounced growth rate reduction during epoxidation than VLB120Δ*C* strains (Table III), resulting in longer biotransformation times (Table II). However, upon organic phase addition, VLB120Δ*C*Δ*ttgV* strains exhibited a much more prominent increase in the specific glucose uptake rate (38%) than VLB120Δ*C* strains (7%; Table III). These results indicate that the constitutive solvent tolerance of the Δ*ttgV* strain comes along with a fundamental change in energy metabolism, not only enabling proton gradient-dependent solvent extrusion but also higher epoxidation activities.

The high epoxidation activities of VLB120 strains during batch cultivation cannot be matched by recombinant *E. coli* JM101.

When cultivated in fed-batch mode, *E. coli* JM101 (pSPZ10) containing StyAB showed higher average productivities and specific epoxidation activities in two-liquid phase biotransformations than *P. taiwanensis* VLB120Δ*C* strains and appeared not to be significantly affected by the degree of glucose limitation (Kuhn et al., 2012a; Kuhn et al., 2013). However, recombinant gene expression levels and specific activities of recombinant *E. coli* have not yet been evaluated under glucose excess conditions, i.e., using a batch mode of cultivation. Given that this strategy substantially improved specific activities and oxygenase expression levels of *P. taiwanensis* VLB120Δ*C* strains, the respective behavior of recombinant *E. coli* JM101 was evaluated. In order to do so, two-liquid phase biotransformations were performed with *E. coli* JM101 (pA-EGFP_B_lac), containing a *styA-eGFP* fusion, cultivated in fed-batch and batch mode.

In contrast to the results obtained with the *P. taiwanensis* strains, both setups resulted in similar maximum specific styrene epoxidations activities of 20-30 U g_{CDW}^{-1}, reached ~2 h after induction (Fig. 4). In both setups, the StyA-eGFP fluorescence further increased and, after 7-8 h of biotransformation, reached levels, which were similar as those observed in batch cultivations of *P. taiwanensis* VLB120Δ*C*Δ*ttgV_AeGFP*. Again, the increase in specific epoxidation activity did not correlate with the increase in oxygenase gene expression, irrespective of the cultivation mode. Batch growth was increasingly affected during biotransformation, although product and acetate concentrations remained below their toxicity limits. This points to a metabolic burden of *styAB* overexpression as it has been observed before (Bühler et al., 2008). In contrast to the VLB120 strains, glucose uptake rates in batch

cultivations did not increase, but rather decreased after organic phase addition (Table III). This coincided with the substantially lower specific epoxidation activities compared to the VLB120 strains. Obviously, the metabolic resources available to simultaneously support high oxygenase levels and activities differ heavily for *E. coli* JM101 and *P. taiwanensis* VLB120, especially during batch cultivation.

Discussion

Constitutive solvent tolerance promoting oxygenase gene expression and activity.

Constitutively solvent-tolerant *P. taiwanensis* VLB120Δ*C*Δ*ttgV* has been shown to exhibit two-fold improved styrene epoxidation activities compared to *P. taiwanensis* VLB120Δ*C* (Volmer et al., 2014; Volmer et al., 2017). The substitution of the *styA* gene with a *styA-eGFP* fusion construct allowed determining the intracellular oxygenase amount and revealed that increased oxygenase levels in the constitutively solvent-tolerant mutant constitute one, but not the only reason for the observed elevated activities. The two strains may further differ in the metabolic capacity for NADH regeneration and/or intracellular styrene and (*S*)-styrene oxide concentrations. The latter may be reduced by the enforced action of the solvent efflux pump TtgGHI in the Δ*ttgV* strain, attenuating substrate and product inhibition of StyAB (Fig. 1; Otto et al., 2004; Ruinatscha, 2009). Attenuation of styrene and (*S*)-styrene oxide toxicity in *P. taiwanensis* VLB120Δ*C*Δ*ttgV* due to constitutive TtgGHI activity may in turn stabilize cell physiology resulting in the observed improvement in *styAB* expression.

Correlation of whole-cell kinetics and two-liquid phase biotransformation performance.

Substrate inhibition kinetics typically asks for controlled substrate supply. In this study, the application of BEHP as extractive organic solvent in fed-batch and batch two-liquid phase biotransformations resulted in aqueous styrene concentrations (0.25

mM), which, according to the substrate inhibition kinetics for resting cells (Fig. 1), theoretically enabled styrene epoxidation activities in the range of 35 and 80 U g_{CDW}^{-1} for the Δ*C* and the Δ*C*Δ*ttgV* strain, respectively. Whereas in the former case, expected activities were reached during fed-batch cultivation in the present (Fig. 2) as well as in former studies (Kuhn et al., 2012a; Park et al., 2007), this was not the case for the constitutively solvent-tolerant Δ*C*Δ*ttgV* strain, which showed the same activity as the Δ*C* strain. During batch cultivation, however, maximal specific styrene epoxidation activities of both the Δ*C* (110 U g_{CDW}^{-1}) and the Δ*C*Δ*ttgV* strains (180 U g_{CDW}^{-1}) were significantly higher than expected from resting-cell kinetics. Thus, resting cell kinetics cannot directly be transferred to cells growing in a two-liquid phase system. This also has been observed for recombinant *E. coli* (Bühler et al., 2006; Park et al., 2006), where direct substrate uptake from the organic phase and biological energy shortage have been identified as the underlying reasons. In case of *P. taiwanensis* VLB120 strains, energy metabolism and oxygenase expression levels played a major role, both depending on growth state and conditions. Energy/ NADH limitation hinders kinetically predicted activities above a certain threshold, possibly explaining the low activities of fed-batch cultivated cells. Overall, VLB120 strains, especially the Δ*ttgV* mutant, were able to boost their epoxidation activity under conditions providing a high energy/ glucose availability, which is in stark contrast to *E. coli* (Fig. 4) and will be further discussed below.

The epoxidation performance of VLB120 strains growing in fed-batch mode is severely limited by glucose availability.

High cell concentrations, as established in case of fed-batch cultivations, can lead to O_2 and styrene mass transfer limitations. However, pO_2 levels were maintained above 20% of saturation (Fig. 2), and no such limitations have been observed at higher feed/ growth rates and higher styrene epoxidation activities of up to 60 U g_{CDW}^{-1} in similar

high-cell density biotransformations with *E. coli* at similar pO_2 levels (Kuhn et al., 2010; Park et al., 2006). Further, a clear correlation of specific activities with the styrene concentration is missing. Thus, limitations by styrene or O_2 can be excluded. The correlation of StyA-eGFP levels with specific activities clearly shows that, for fed-batch cultivated cells, increasing oxygenase levels did not translate in increasing epoxidation activities, which remained low for both VLB120 strains (Fig. 5). Intracellular oxygenase levels were thus not limiting either. Rather, a correlation of activities with the gradual increase in glucose limitation due to the constant glucose feed rate at increasing cell concentrations can be inferred. Such increasing glucose limitation resulted in a continuous decrease of glucose uptake rates during biotransformation (from 2.30 to 1.12 and from 2.23 to 1.44 mmol g^{-1} h^{-1} for VLB120Δ*C_AeGFP* and VLB120Δ*C*Δ*ttgV_AeGFP*, respectively). Beside the decrease in growth and glucose uptake rates, the decrease of the specific epoxidation rates can thus also be considered a result of decreasing glucose availability, which additionally may have affected other energy-dependent processes such as recombinant gene expression and solvent tolerance. These considerations indicate that the strongly decreased styrene epoxidation activities and slightly lower oxygenase levels of the *Pseudomonas* strains during fed-batch as compared to batch cultivations are caused by glucose and thus energy limitation.

Glucose excess conditions afford VLB120 strains high epoxidation activities, which appear to correlate with the strain-inherent metabolic capacity.

In batch cultivations, specific styrene epoxidation activities correlated linearly to intracellular StyA-eGFP levels up to maxima of ~110 and ~170-180 U g_{CDW}^{-1} for *P. taiwanensis* VLB120Δ*C_AeGFP* and its Δ*ttgV* derivative, respectively (Fig. 5). These maximum activities were reached after ~3 h of biotransformation/ induction (Figs. 2 and 3). By then, the specific activities thus appeared to be limited by the intracellular

styrene monooxygenase concentration. The further increase in StyA-eGFP levels did not translate into a further activity increase. Specific epoxidation rates remained constant. A similar behavior was observed with plasmid-based *styA-eGFP* gene expression in solvent-tolerant *P. putida* DOT-T1E (Lindmeyer et al., 2015a; Lindmeyer et al., 2015b). In the later stage of biotransformations with batch-cultivated VLB120 strains, beside styrene and O_2 availabilities, the intracellular oxygenase level again can be excluded as limiting factor. Thus, NADH regeneration via glucose catabolism remains the only possible limitation. However, *ttgV* deletion and the resulting constitutive solvent tolerance obviously led to changes in metabolic network operation (more pronounced increase and decrease in specific glucose uptake and growth rates, respectively, Table III), thereby significantly enhancing the styrene epoxidation capacity of the VLB120 strain. On the one hand, this may be ascribed to reduced toxification effects having a beneficial effect on NADH availability/ regeneration. On the other hand, solvent-tolerant *Pseudomonas* strains have been reported to boost their metabolic capacity upon adaptation to the presence of toxic solvents, in order to provide the energy required to operate solvent tolerance mechanisms (Blank et al., 2008b; Segura et al., 2005; Volkers et al., 2006; Volkers et al., 2015). Thus, the regulator TtgV, of which the knockout enabled constitutive solvent tolerance (Volmer et al., 2014; Volmer et al., 2017), may, beside the inhibition of efflux pump gene expression, also be involved in the regulation of the energy metabolism. As a consequence its knockout enabled a higher metabolic capacity and thus higher epoxidation activities under glucose excess conditions.

***P. taiwanensis* VLB120Δ*ttgV* – a host for highly efficient oxyfunctionalization.**

The central carbon metabolism of Pseudomonads is naturally geared to generate plenty of reductive power, i.e., NAD(P)H, which makes these bacteria highly promising hosts for redox-intensive reactions (Nikel and de Lorenzo, 2018). This is

confirmed by the high specific epoxidation activities obtained with *P. taiwanensis* VLB120Δ*C*Δ*ttgV* strains, which are unrivaled so far for NAD(P)H-dependent microbial oxygenation under process conditions (Blank et al., 2010; Schrewe et al., 2013; Volmer et al., 2017). Activities in the same range have been reported for the oxygenase-initiated degradation of hydrocarbons such as xylene (170 U g_{CDW}^{-1}) or styrene (200 U g_{CDW}^{-1}), which, however, did not involve product accumulation (Duetz et al., 1997; Nöthe and Hartmans, 1994). Via directed evolution of the styrene monooxygenase from *P. putida* CA-3, Gursky *et al.* increased short-term resting-cell activities of recombinant *E. coli* BL21 from 21 to impressive 266 U g_{CDW}^{-1} (Gursky et al., 2010). The high (*S*)-styrene oxide formation activity was, however, accompanied by pronounced phenylacetaldehyde accumulation (30-35% of total product). With recombinant *E. coli* producing the styrene monooxygenase of *P. putida* SN1, co-expression of *groEL-ES* and *dnaK-dnaJ-grpE* chaperone genes enabled styrene epoxidation activities of up to 180 and 106 U g_{CDW}^{-1} in resting-cell assays and bioreactor-based two-liquid phase biotransformations, respectively (Bae et al., 2010). For VLB120 StyAB, the highest activities achieved so far with recombinant *E. coli* under process conditions amount to 130 U g_{CDW}^{-1} and were based on resting cells (Julsing et al., 2012). However, a better process performance has been achieved with growing cells of recombinant *E. coli* and the VLB120Δ*C* strain with lower maximal activities (30-60 U g_{CDW}^{-1}, Kuhn et al., 2012a; Kuhn et al., 2012b) and was not reached with resting cells due to their lower robustness resulting in lower process stability. The exceptionally high activity and robustness of *P. taiwanensis* VLB120Δ*C*Δ*ttgV* under process conditions allows an improvement of several important process performance parameters (Table II). Beside the high activity, the high (*S*)-styrene oxide yields on glucose and biomass during batch growth illustrate the immense potential of the constitutively solvent-tolerant strain. These yields were

1.7 and 2.8-fold higher, respectively, compared to those obtained with recombinant *E. coli*, of which the performance has been assessed to be competitive to existing chemical alternatives (Kuhn et al., 2010). The lower overall average productivities compared to those achieved in fed-batch setups (Kuhn et al., 2012a; Kuhn et al., 2010) can be explained by the 7- to 20-fold lower cell concentration in the batch cultures evaluated in this study. A high-cell density cultivation setup involving excess glucose conditions thus appears to be a promising approach to reach high overall productivities as well as yields on glucose and biomass. Remarkably, no decrease in specific activity occurred in the batch setup unless glucose was depleted.

In conclusion, the extraordinarily high specific activities of constitutively solvent-tolerant *P. taiwanensis* VLB120Δ*C*Δ*ttgV* growing under glucose excess conditions can be attributed to its high metabolic capacity, which also enabled high expression levels. This together with high product yields on glucose and biomass qualifies the VLB120Δ*C*Δ*ttgV* strain as a highly attractive tool for the development of eco-efficient oxyfunctionalization processes.

References

Bae JW, Doo EH, Shin SH, Lee SG, Jeong YJ, Park JB, Park S. 2010. Development of a recombinant *Escherichia coli*-based biocatalyst to enable high styrene epoxidation activity with high product yield on energy source. Process Biochemistry 45(2): 147-152.

Bertani G. 1951. Studies on lysogenesis I. The mode of phage liberation by lysogenic *Escherichia coli*. Journal of Bacteriology 62(3): 293-300.

Besse P, Veschambre H. 1994. Chemical and biological synthesis of chiral epoxides. Tetrahedron 50: 8885-8927.

Blank LM, Ebert BE, Bühler B, Schmid A. 2008a. Metabolic capacity estimation of *Escherichia coli* as a platform for redox biocatalysis: constraint-based modeling and experimental verification. Biotechnology and Bioengineering 100(6): 1050-1065.

Blank LM, Ionidis G, Ebert BE, Bühler B, Schmid A. 2008b. Metabolic response of *Pseudomonas putida* during redox biocatalysis in the presence of a second octanol phase. FEBS Journal 275(20): 5173-5190.

Blank LM, Ebert BE, Buehler K, Bühler B. 2010. Redox biocatalysis and metabolism: Molecular mechanisms and metabolic network analysis. Antioxidants & Redox Signaling 13(3): 349-394.

Bühler B, Bollhalder I, Hauer B, Witholt B, Schmid A. 2003. Use of the two-liquid phase concept to exploit kinetically controlled multistep biocatalysis. Biotechnology and Bioengineering 81(6): 683-694.

Bühler B, Park JB, Blank LM, Schmid A. 2008. NADH availability limits asymmetric biocatalytic epoxidation in growing recombinant *Escherichia coli*. Applied and Environmental Microbiology 74(5): 1436-1446.

Bühler B, Straathof AJJ, Witholt B, Schmid A. 2006. Analysis of two-liquid-phase multistep biooxidation based on a process model: Indications for biological energy shortage. Organic Process Research & Development 10(3): 628-643.

Clomburg JM, Crumbley AM, Gonzalez R. 2017. Industrial biomanufacturing: The future of chemical production. Science 355: eaag0804.

Copeland RA. 2000. *Enzymes: A practical introduction to structure, mechanism, and data analysis*; Wiley-VCH, Inc., New York, USA.

Cornish-Bowden A. 1995. *Analysis of enzyme kinetic data*; Oxford University Press, Oxford, UK and New York, USA.

Duetz WA, Wind B, Kamp M, van Andel JF. 1997. Effect of growth rate, nutrient limitation and succinate on expression of TOL pathway enzymes in response to m-xylene in chemostat cultures of *Pseudomonas putida* (pWW0). Microbiology 143: 2331-2338.

Gursky LJ, Nikodinovic-Runic J, Feenstra KA, O'Connor KE. 2010. *In vitro* evolution of styrene monooxygenase from *Pseudomonas putida* CA-3 for improved epoxide synthesis. Applied Microbiology and Biotechnology 85(4): 995-1004.

Halan B, Schmid A, Buehler K. 2010. Maximizing the productivity of catalytic biofilms on solid supports in membrane aerated reactors. Biotechnology and Bioengineering 106(4): 516-527.

Heipieper HJ, Neumann G, Cornelissen S, Meinhardt F. 2007. Solvent-tolerant bacteria for biotransformations in two-phase fermentation systems. Applied Microbiology and Biotechnology 74(5): 961-973.

Hofstetter K, Lutz J, Lang I, Witholt B, Schmid A. 2004. Coupling of biocatalytic asymmetric epoxidation with NADH regeneration in organic-aqueous emulsions. Angewandte Chemie International Edition 43(16): 2163-2166.

Isken S, Derks A, Wolffs PFG, de Bont JAM. 1999. Effect of organic solvents on the yield of solvent-tolerant *Pseudomonas putida* S12. Applied and Environmental Microbiology 65(6): 2631-2635.

Jahn M, Vorpahl C, Turkowsky D, Lindmeyer M, Bühler B, Harms H, Müller S. 2014. Accurate determination of plasmid copy number of flow-sorted cells using droplet digital PCR. Analytical Chemistry 86(12): 5969-5976.

Julsing MK, Kuhn D, Schmid A, Bühler B. 2012. Resting cells of recombinant *E. coli* show high epoxidation yields on energy source and high sensitivity to product inhibition. Biotechnology and Bioengineering 109(5): 1109-1119.

Köhler KAK, Rückert C, Schatschneider S, Vorhölter F, Sczepanowski R, Blank LM, Niehaus K, Goesmann A, Pühler A, Kalinowski J, Schmid A. 2013. Complete genome sequence of *Pseudomonas* sp. strain VLB120 a solvent tolerant, styrene degrading bacterium, isolated from forest soil. Journal of Biotechnology 168(4): 729-730.

Kuhn D, Bühler B, Schmid A. 2012a. Production host selection for asymmetric styrene epoxidation: *Escherichia coli* vs. solvent-tolerant *Pseudomonas*. Journal of Industrial Microbiology and Biotechnology 39(8): 1125-1133.

Kuhn D, Fritzsch FSO, Zhang X, Wendisch VF, Blank LM, Bühler B, Schmid A. 2013. Subtoxic product levels limit the epoxidation capacity of recombinant *E. coli* by increasing microbial energy demands. Journal of Biotechnology 163(2): 194-203.

Kuhn D, Julsing MK, Heinzle E, Bühler B. 2012b. Systematic optimization of a biocatalytic two-liquid phase oxyfunctionalization process guided by ecological and economic assessment. Green Chemistry 14(3): 645-653.

Kuhn D, Kholiq MA, Heinzle E, Bühler B, Schmid A. 2010. Intensification and economic and ecological assessment of a biocatalytic oxyfunctionalization process. Green Chemistry 12(5): 815-827.

Lim HN, Lee Y, Hussein R. 2011. Fundamental relationship between operon organization and gene expression. Proceedings of the National Academy of Sciences of the United States of America 108(26): 10626-10631.

Lindmeyer M. 2016. *Pseudomonas and heterogeneity - benefits and challenges for strain and process engineering*. PhD thesis. TU Dortmund University, Dortmund.

Lindmeyer M, Jahn M, Vorpahl C, Müller S, Schmid A, Bühler B. 2015a. Variability in subpopulation formation propagates into biocatalytic variability of engineered *Pseudomonas putida* strains. Frontiers in Microbiology 6: 1042.

Lindmeyer M, Meyer D, Kuhn D, Bühler B, Schmid A. 2015b. Making variability less variable: matching expression system and host for oxygenase-based biotransformations. Journal of Industrial Microbiology and Biotechnology 42(6): 851-866.

Martinez-Garcia E, de Lorenzo V. 2011. Engineering multiple genomic deletions in Gram-negative bacteria: analysis of the multi-resistant antibiotic profile of *Pseudomonas putida* KT2440. Environmental Microbiology 13(10): 2702-2716.

Messing J. 1979. A multipurpose cloning system based on the single-stranded DNA bacteriophage M13. Recombinant DNA Technical Bulletin 3(2): 43-49.

Meyer D, Bühler B, Schmid A. 2006. Process and catalyst design objectives for specific redox biocatalysis. Advances in Applied Microbiology 59: 53-91.

Nikel PI, de Lorenzo, V. 2018. *Pseudomonas putida* as a functional *chassis* for industrial biocatalysis: From native biochemistry to *trans*-metabolism. Metabolic Engineering 50: 142-155.

Nöthe C, Hartmans S. 1994. Formation and degradation of styrene oxide stereoisomers by different microorganisms. Biocatalysis 10(1-4): 219-225.

Otto K, Hofstetter K, Röthlisberger M, Witholt B, Schmid A. 2004. Biochemical characterization of StyAB from *Pseudomonas* sp. strain VLB120 as a two-component flavin-diffusible monooxygenase. Journal of Bacteriology 186(16): 5292-5302.

Panke S, Held M, Wubbolts MG, Witholt B, Schmid A. 2002. Pilot-scale production of (*S*)-styrene oxide from styrene by recombinant *Escherichia coli* synthesizing styrene monooxygenase. Biotechnology and Bioengineering 80(1): 33-41.

Panke S, Meyer A, Huber CM, Witholt B, Wubbolts MG. 1999. An alkane-responsive expression system for the production of fine chemicals. Applied and Environmental Microbiology 65(6): 2324-2332.

Panke S, Witholt B, Schmid A, Wubbolts MG. 1998. Towards a biocatalyst for (*S*)-styrene oxide production: characterization of the styrene degradation pathway of *Pseudomonas* sp. strain VLB120. Applied and Environmental Microbiology 64(6): 2032-2043.

Panke S, Wubbolts MG, Schmid A, Witholt B. 2000. Production of enantiopure styrene oxide by recombinant *Escherichia coli* synthesizing a two-component styrene monooxygenase. Biotechnology and Bioengineering 69(1): 91-100.

Park JB, Bühler B, Habicher T, Hauer B, Panke S, Witholt B, Schmid A. 2006. The efficiency of recombinant *Escherichia coli* as biocatalyst for stereospecific epoxidation. Biotechnology and Bioengineering 95(3): 501-512.

Park JB, Bühler B, Panke S, Witholt B, Schmid A. 2007. Carbon metabolism and product inhibition determine the epoxidation efficiency of solvent-tolerant *Pseudomonas* sp. strain VLB120Δ*C*. Biotechnology and Bioengineering 98(6): 1219-1229.

Riesenberg D, Schulz V, Knorre WA, Pohl HD, Korz D, Sanders EA, Ross A, Deckwer WD. 1991. High cell density cultivation of *Escherichia coli* at controlled specific growth rate. Journal of Biotechnology 20(1): 17-28.

Ruinatscha R. 2009. *Asymmetric biocatalytic epoxidation in a scalable electrochemical reactor using FAD-dependent styrene monooxygenase*. PhD thesis. TU Dortmund, Dortmund.

Sambrook J, Russel DW. 2001. *Molecular cloning: a laboratory manual*; Cold Spring Harbor Laboratory Press, Cold Spring Harbor, NY.

Schmid A, Hofstetter K, Feiten HJ, Hollmann F, Witholt B. 2001. Integrated biocatalytic synthesis on gram scale: The highly enantio selective preparation of chiral oxiranes with styrene monooxygenase. Advanced Synthesis and Catalysis 343(6-7): 732-737.

Schrewe M, Julsing MK, Bühler B, Schmid A. 2013. Whole-cell biocatalysis for selective and productive C-O functional group introduction and modification. Chemical Society Reviews 42(15): 6346-6377.

Segura A, Godoy P, van Dillewijn P, Hurtado A, Arroyo N, Santacruz S, Ramos JL. 2005. Proteomic analysis reveals the participation of energy- and stress-related proteins in the response of *P. putida* DOT-T1E to toluene. Journal of Bacteriology 187(17): 5937-5945.

Sheldon RA, Woodley JM. 2017. Role of biocatalysis in sustainable chemistry. Chemical Reviews 118(2): 801-838.

Volkers RJM, de Jong AL, Hulst AG, van Baar BLM, de Bont JAM, Wery J. 2006. Chemostat-based proteomic analysis of toluene-affected *P. putida* S12. Environmental Microbiology 8(9): 1674-1679.

Volkers RJM, Snoek LB, Ruijssenaars HJ, de Winde JH. 2015. Dynamic response of Pseudomonas putida S12 to sudden addition of toluene and the potential role of the solvent rolerance gene *trgI*. PLOS ONE 10(7): e0132416.

Volmer J, Neumann C, Bühler B, Schmid A. 2014. Engineering of *Pseudomonas taiwanensis* VLB120 for constitutive solvent tolerance and increased specific styrene epoxidation activity. Applied and Environmental Microbiology 80(20): 6539-6548.

Volmer J, Schmid A, Bühler B. 2017. The application of constitutively solvent-tolerant *P. taiwanensis* VLB120ΔCΔttgV for stereospecific epoxidation of toxic styrene alleviates carrier solvent use. Biotechnology Journal.

Woodley JM, Breuer M, Mink D. 2013. A future perspective on the role of industrial biotechnology for chemicals production. Chemical Engineering Research and Design 91(10): 2029-2036.

Figures

Figure 1. Substrate inhibition kinetics of styrene epoxidation catalyzed by the *P. taiwanensis* strains VLB120Δ*C* and VLB120Δ*C*Δ*ttgV*. Specific activities at different substrate concentrations were determined in resting-cell activity assays with 5 min reaction time carried out in 0.1 M potassium phosphate buffer (pH 7.4) containing 1% (w/v) glucose. Substrate inhibition curves and whole-cell kinetic parameters were fitted with Equation 1 using a least-square fit algorithm to perform nonlinear regression with GraphPad Prism 6.05.

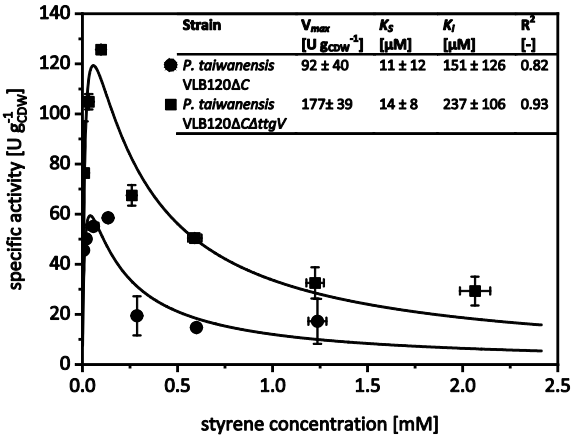

Figure 2. Bioreactor-based two-liquid phase styrene biotransformations with the *P. taiwanensis* strains VLB120Δ*C_AeGFP* (A and B) and VLB120Δ*C*Δ*ttgV_AeGFP* (C and D) cultivated in fed-batch mode in 1 L RB medium. At t = -13 h, fed-batch cultivation involved exponential glucose feeding to support a growth rate of μ = 0.1 h^{-1}. Biotransformations were started at t = 0 by the addition of well mixed BEHP (920 mL) and styrene (80 mL). After organic phase addition, the feed rate was kept constant at 7.8 g_{Glc} h^{-1}. Panels A and C show the time courses of dissolved oxygen (pO_2), biomass, glucose, and gluconate concentrations and the glucose feed rate. Panels B and D show the time courses of styrene and (*S*)-styrene oxide concentrations in the organic phase, specific activities, and specific fluorescence levels corresponding to intracellular StyA-eGFP concentrations.

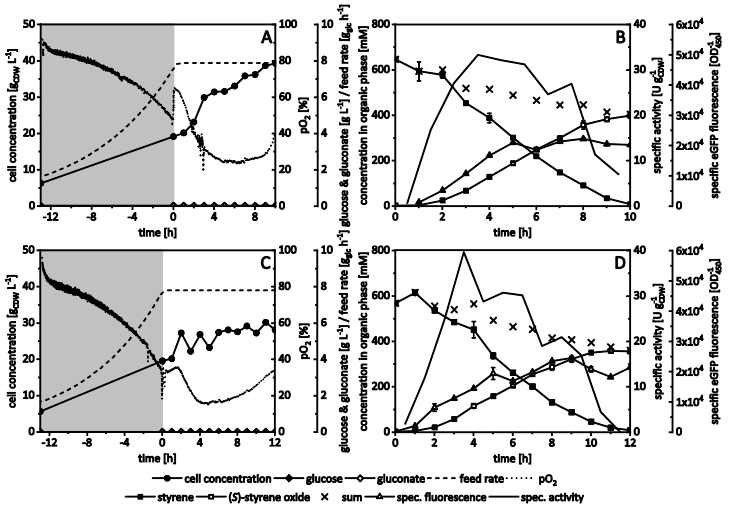

Figure 3. Bioreactor-based two-liquid phase styrene biotransformations with the *P. taiwanensis* strains VLB120Δ*C_AeGFP* (A and B) and VLB120ΔCΔ*ttgV_AeGFP* (C and D) cultivated in batch mode in 1 L RB medium. Biotransformations were started at t = 0 by adding well mixed BEHP (920 mL) and styrene (80 mL). Panels A and C show the time courses of dissolved oxygen (pO_2), biomass, glucose, and gluconate concentrations. Panels B and D show the time courses of styrene and (*S*)-styrene oxide concentrations in the organic phase, specific activities, and specific fluorescence levels corresponding to intracellular StyA-eGFP concentrations.

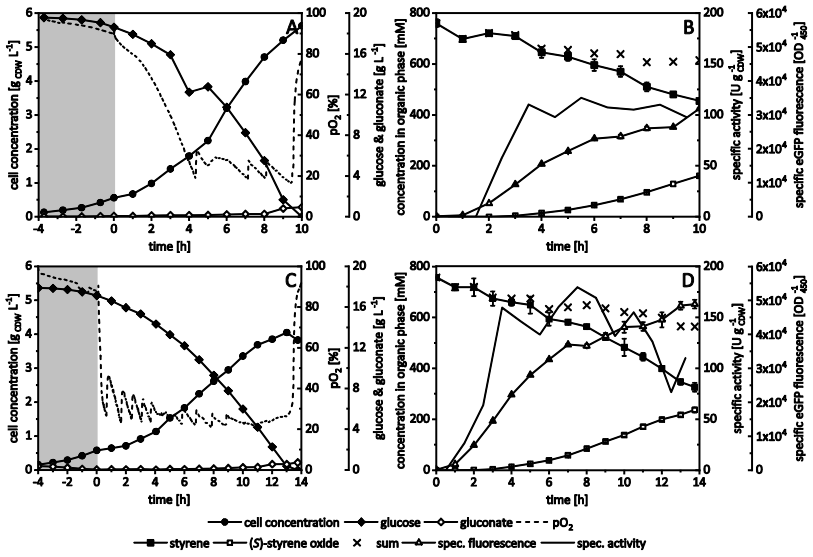

Figure 4. Bioreactor-based two-liquid phase styrene biotransformations with *E. coli* JM101 (pA-EGFP_B_lac) cultivated in batch (**A** + **B**) and fed-batch (**C** + **D**) mode. At the time point 0 h, biotransformations were started by adding well mixed 920 mL BEHP and 80 mL styrene and 1 mM IPTG as induction agent. Panels **A** and **C** show the courses of styrene and (*S*)-styrene oxide concentrations in the organic phase, specific activities, and specific fluorescence levels corresponding to intracellular StyA-eGFP concentrations. Panels **B** and **D** illustrate the courses of dissolved oxygen (pO_2), biomass, glucose, and acetate concentrations and of the feed rate in case of fed-batch cultivation.

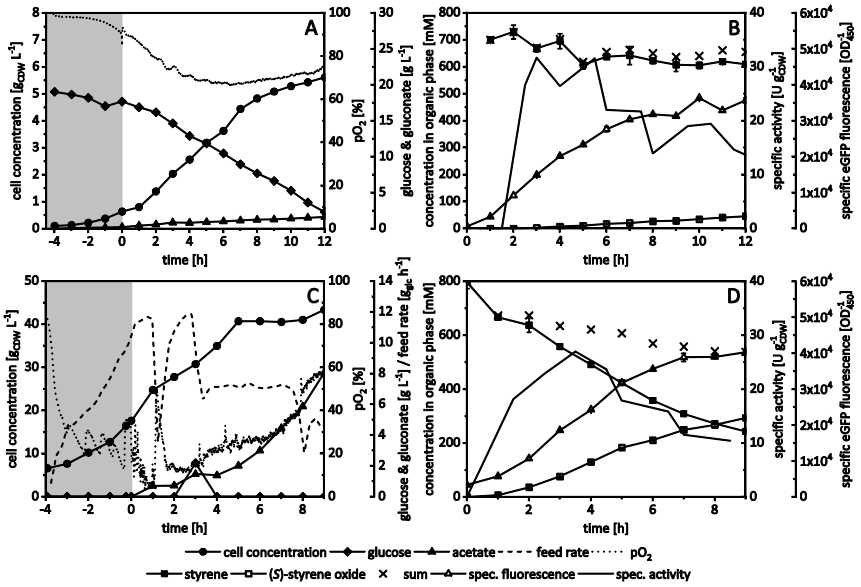

Figure 5. Correlation between specific styrene epoxidation activities and specific eGFP fluorescence levels in two-liquid phase biotransformations with the *P. taiwanensis* strains VLB120Δ*C_AeGFP* and VLB120Δ*C*Δ*ttgV_AeGFP* growing in fed-batch and batch mode. The data points given correspond to the data given in Figs. 2 and 3 except in case of *P. taiwanensis* VLB120Δ*C*Δ*ttgV_AeGFP* batch cultivations, for which the average values of 3 independent biotransformations are given. Area I: Glucose limitation during fed-batch biotransformations limits maximum specific activities and the oxygenase expression level in both strains. Area II: Glucose excess during batch cultivation of *P. taiwanensis* VLB120Δ*C_AeGFP* results in increased maximum specific epoxidation activities and oxygenase expression levels. Area III: The constitutive solvent tolerance of *P. taiwanensis* VLB120Δ*C*Δ*ttgV_AeGFP* results in a further increase of maximum specific activities and oxygenase expression levels.

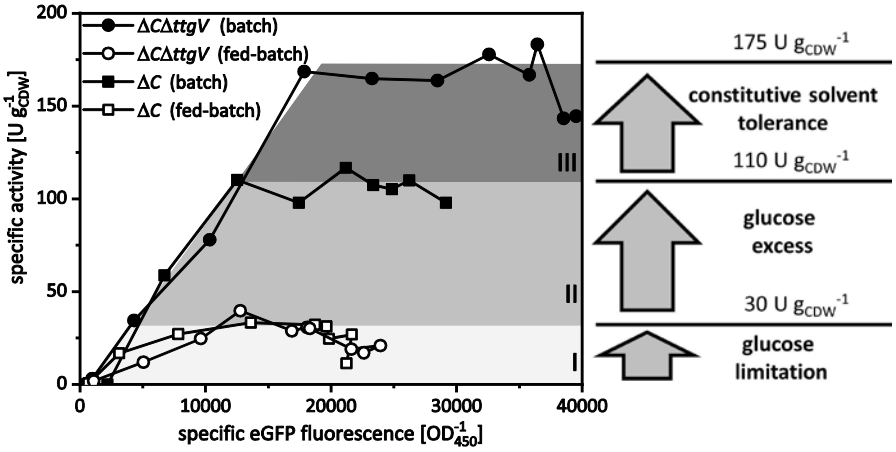

Table I. Bacterial strains and plasmids used in this study

Strain	Characteristics	Reference
P. taiwanensis VLB120Δ*C*	*styC*-deficient mutant of *P. taiwanensis* VLB120 (*styC* disrupted by Sm^r gene), Sm^r	(Park et al., 2007)
P. taiwanensis VLB120Δ*C*Δ*ttgV*	*ttgV*-deficient mutant of *P. taiwanensis* VLB120Δ*C*, Sm^r	(Volmer et al., 2014)
P. taiwanensis VLB120Δ*C_AeGFP*	*P. taiwanensis* VLB120Δ*C* containing a *styA-eGFP* fusion on the megaplasmid pSTY, Sm^r	This study
P. taiwanensis VLB120Δ*C*Δ*ttgV_AeGFP*	*P. taiwanensis* VLB120Δ*C*Δ*ttgV* containing a *styA-eGFP* fusion on the megaplasmid pSTY, Sm^r	This study
E. coli DH5α λpir	λ-pir lysogen derivate of *E. coli* DH5α	(Martinez-Garcia et al., 2011)
E. coli JM101	*supE thi*-1 Δ(*lac-proAB*) F'[*traD36 proAB*$^+$ *lac*I^q *lacZ* ΔM15]	(Messing, 1979)
Plasmid	**Characteristics**	**Reference**
pSMART-HCKan_StyA-eGFPB	pSMART[a]-derived, bearing a 3,033 bp fragment containing *styA-eGFP* and *styB*, Km^r	(Jahn et al., 2014)
pEMG	*ori*R6K, *ori*T, *lacZα* with two flanking I-*Sce*I sites, Km^r	(Martinez-Garcia et al., 2011)
pEMG-A-eGFPB	pEMG backbone, bearing a 2,078 bp fragment for knock-in of *styA-eGFP styB*, Km^r	This study
pSW-2	*ori*RK2/*trfA*, (*xylS*, P_m), Gm^r,	(Martinez-Garcia et al., 2011)
pA-EGFP_B_lac	pCom10-derived, *lac*-regulatory system (*lac*I, P_{lacUV5}), *styA-eGFP*, *styB*, Km^r	(Jahn et al., 2014; Lindmeyer et al., 2015b)

Sm^r: streptomycin resistance, Km^r: kanamycin resistance, Gm^r: gentamycin resistance
[a] Lucigen (Middleton, USA)

Table II. Process parameters of biotransformations with *P. taiwanensis* VLB120 strains in batch and fed-batch two-liquid phase bioreactor setups.

		Fed-batch		Batch	
		P. taiwanensis VLB120			
Process parameter	Unit	Δ*C_AeGFP*	Δ*C*Δ*ttgV_AeGFP*	Δ*C_AeGFP*	Δ*C*Δ*ttgV_AeGFP*
Biotransformation time	h	10.00	12.00	10.00	13.75
Initial styrene conc.	mM	643.60	611.75	760.57	757.79
Final styrene conc.	mM	5.70	5.72	454.89	327.05

Final (*S*)-styrene oxide conc.	mM	396.40	353.01	160.94	237.57
Cell concentration at start of biotransformation	$g_{CDW}\ L_{aq}^{-1}$	19.01	19.43	0.57	0.58
Maximal cell concentration	$g_{CDW}\ L_{aq}^{-1}$	39.13	30.02	5.63	3.83
Glucose consumed during biotransformation	g	78.56	93.53	18.62	17.13
Average productivity	$g\ L_{tot}^{-1}\ h^{-1}$	2.38	1.77	0.97	1.04
Maximal specific epoxidation activity	$U\ g_{CDW}^{-1}$	33	40	110	180
Maximal specific fluorescence intensity	OD_{450}^{-1}	$2 \cdot 10^4$	$2 \cdot 10^4$	$3 \cdot 10^4$	$5 \cdot 10^4$
Specific fluorescence intensity at maximal activity	OD_{450}^{-1}	$1.0 \cdot 10^4$	$1.0 \cdot 10^4$	$0.95 \cdot 10^4$	$1.45 \cdot 10^4$
Biomass yield[a]	$g_{CDW}\ g_{Glc}^{-1}$	0.26	0.11	0.27	0.19
(*S*)-styrene oxide yield[b]	$g_{SO}\ g_{Glc}^{-1}$	0.61	0.45	1.04	1.67
(*S*)-styrene oxide yield[c]	$g_{SO}\ g_{CDW}^{-1}$	1.22	1.41	3.43	7.45

[a] Biomass yield on glucose during biotransformation

[b] (*S*)-styrene oxide yield on glucose during biotransformation

[c] (*S*)-styrene oxide yield on biomass for entire process.

Table III. Specific growth (μ) and glucose uptake (r_{Glc}) rates of *P. taiwanensis* and *E. coli* strains in batch biotransformations.

	Growth rate μ [h^{-1}]		Glc uptake rate r_{Glc} [mmol g^{-1} h^{-1}]	
Strain	Before organic phase addition	After organic phase addition	Before organic phase addition	After organic phase addition
P. taiwanensis				
VLB120Δ*C_AeGFP*	0.39	0.30	5.09	5.47
VLB120Δ*C*Δ*ttgV_AeGFP*	0.33	0.22	3.49	4.82
E. coli JM101				
pA-EGFP_B_lac	0.53	0.37	5.76	5.12